

Facet-specific photoreduction and immobilization of Cr(VI) on hematite nanocrystals

Chaorong Chen ^{a, b, f}, Haiyang Xian ^{a, b}, Jing Liu ^c, Qingze Chen ^{a, b}, Xiaoliang Liang ^{a, b}, Runliang Zhu ^{a, b*}, Michael F. Hochella Jr. ^{d, e}

^a *CAS Key Laboratory of Mineralogy and Metallogeny, Guangdong Provincial Key Laboratory of Mineral Physics and Materials, Guangzhou Institute of Geochemistry, Chinese Academy of Sciences (CAS), Guangzhou 510640, China*

^b *University of Chinese Academy of Sciences, Beijing 100049, China*

^c *State Key Laboratory of Lunar and Planetary Sciences, Macau University of Science and Technology, Taipa 999078, Macau, China*

^d *Energy and Environment Directorate, Pacific Northwest National Laboratory, Richland, WA 99354, USA*

^e *Department of Geosciences, Virginia Tech, Blacksburg, VA 24061, USA*

^f *Department of Environment, College of Environment and Resources, Xiangtan University, Xiangtan, 411105, China*

* Corresponding author

Phone: 86-020-85297603

Fax: 86-020-85297603

E-mail: zhurl@gig.ac.cn

Fig. S1. SEM images of HNPs (a) and HNCs (b).

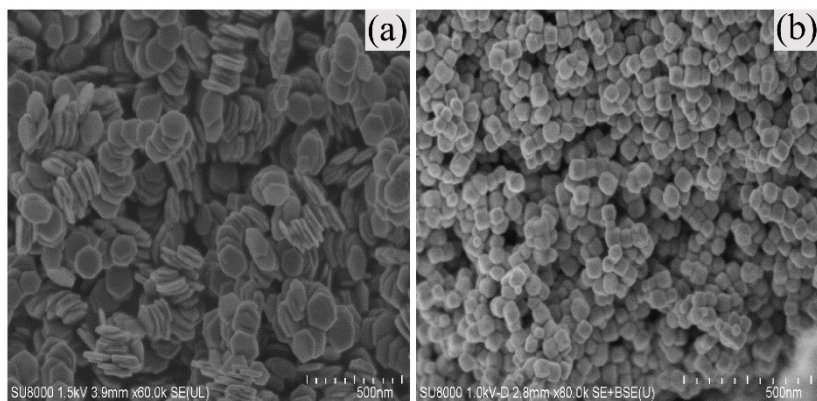


Fig. S2. N₂ adsorption/desorption curves of HNPs (a) and HNCs (b); Tauc plots of HNPs and HNCs (c)

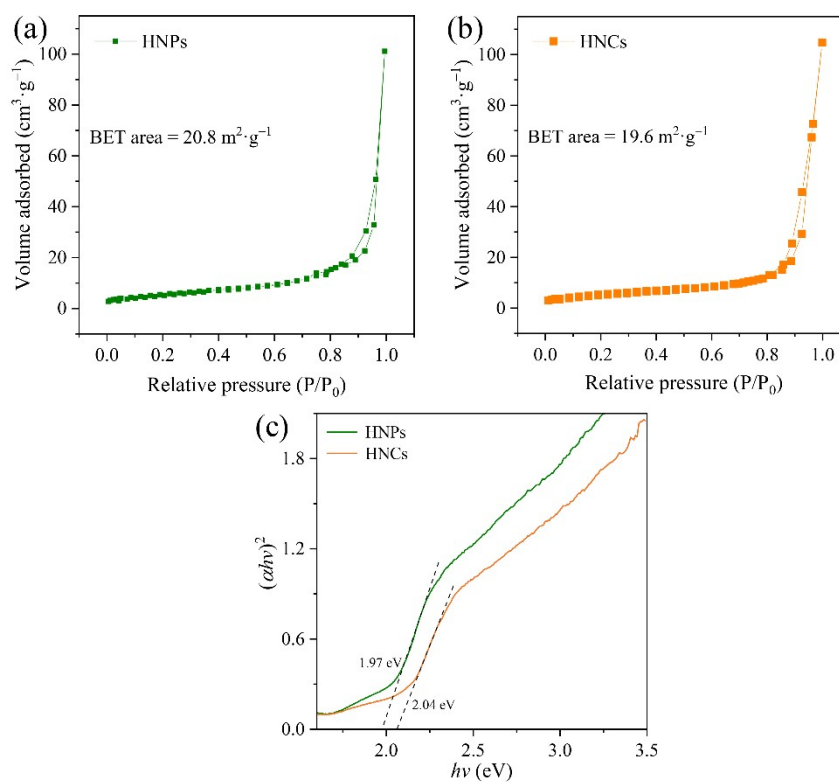
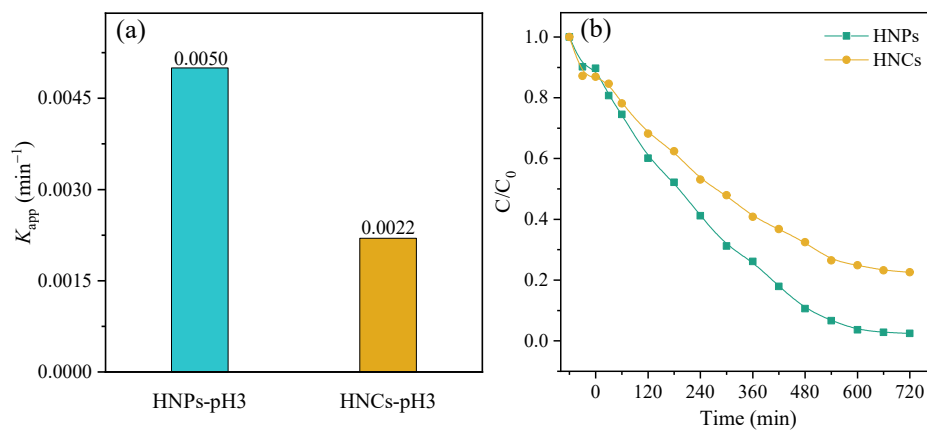


Fig. S3. (a) apparent reaction rate constant (K_{app}) for the reduction of Cr(VI) by HNPs and HNCs at pH 3; (b) The removal kinetics of Cr(VI) on HNPs and HNCs at pH 3 after 720 min (approaches reaction equilibrium).



720 min (approaches reaction equilibrium).

Fig. S4. XPS spectra of Cr 2p_{3/2} for HNPs (a,b) and HNCs (c,d) after reaction at pH 4 and 5, respectively.

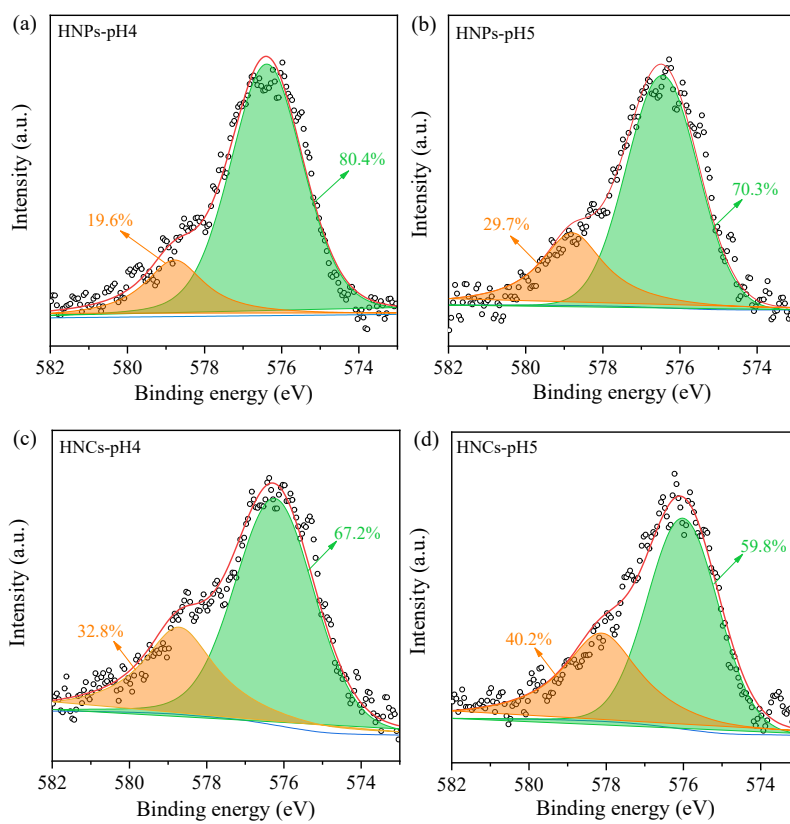


Fig. S5. Concentration of Cr(VI) and total Cr in solution after reaction at different initial pH.

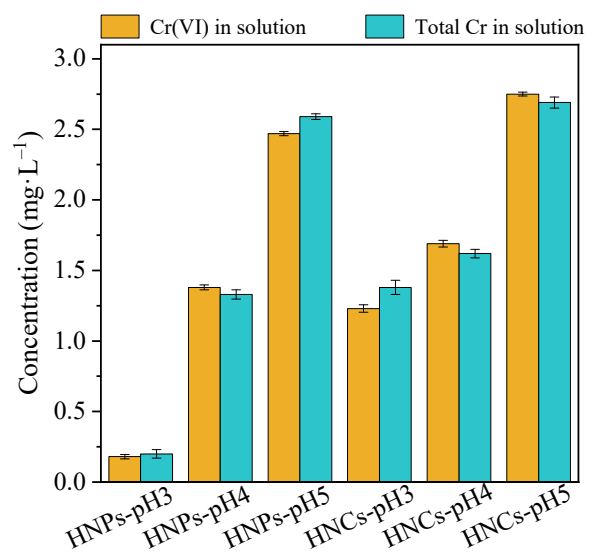


Fig. S6. EDS spectra of HNPs and HNCs after reaction at pH 3.

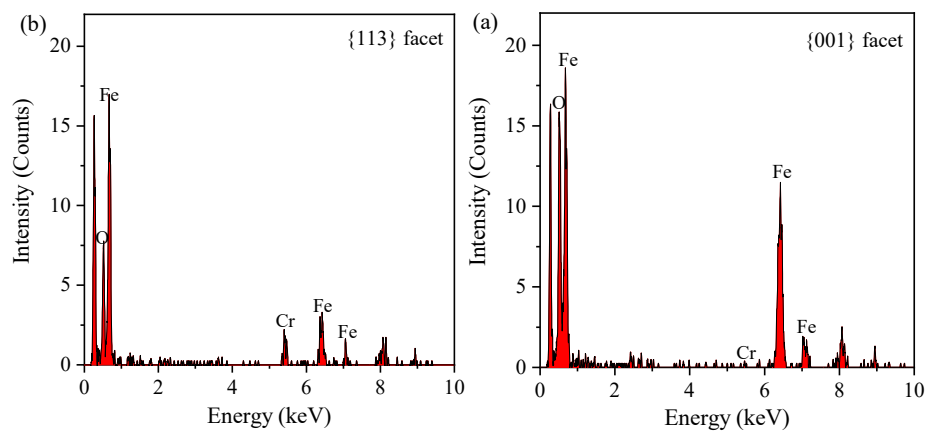


Fig. S7. (a) HAADF-STEM image of HNPs, (b) EELS spectra of the two samples extracted from the marked area in the STEM images.

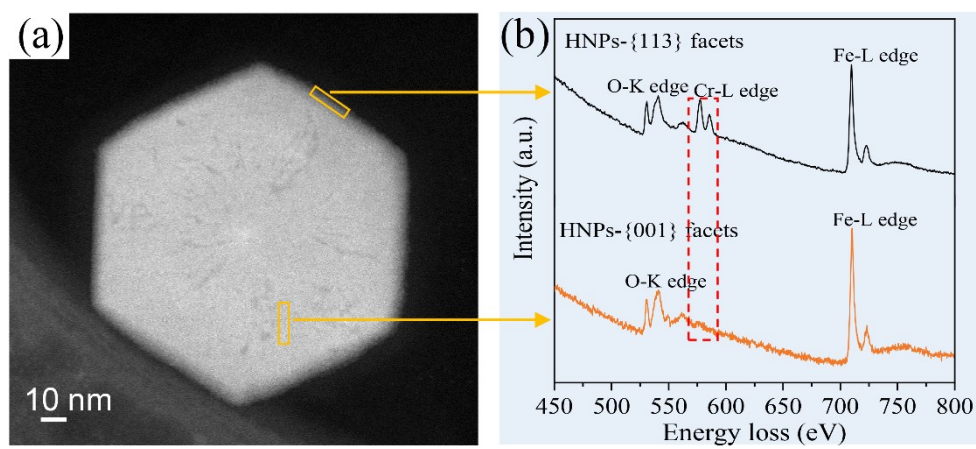


Fig. S8. Desorption of the Cr(VI) and total Cr that immobilized by HNPs or HNCs in the dark versus under light irradiation

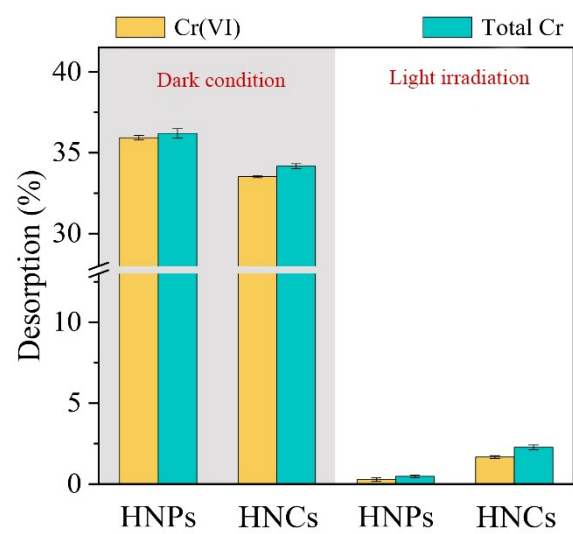


Fig. S9. Calculated electrostatic potentials for (a) $\{001\}$ and (b) $\{113\}$ facets (the bottom cartoons are the DFT-optimized structure model of the corresponding facets).

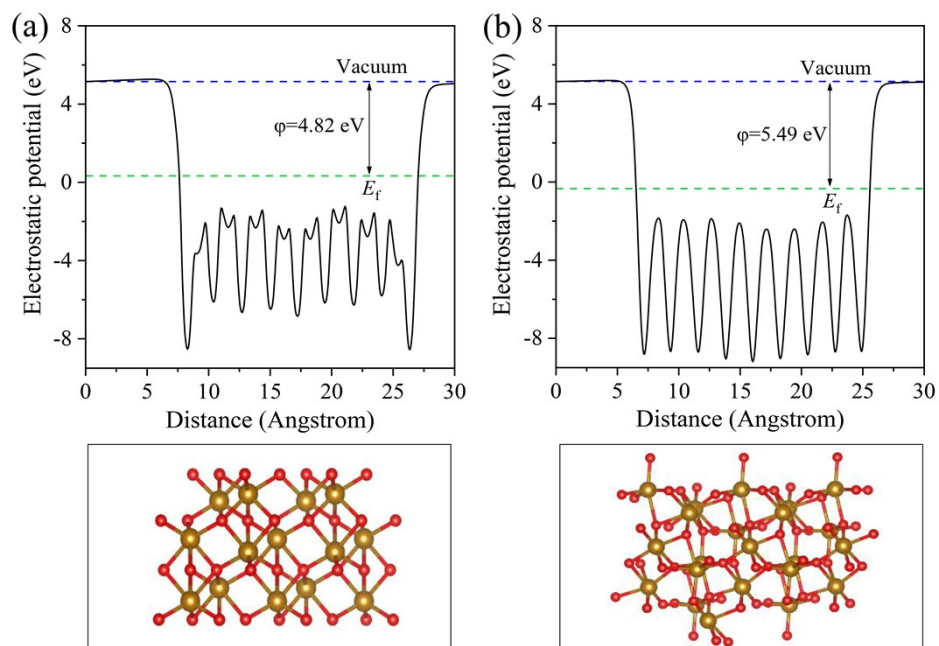


Fig. S10. (a) Radical quenching experiments during Cr(VI) reduction over HNPs and HNCs under light irradiation; (b) ESR spectra of DMPO- $\bullet\text{O}_2^-$ in the HNPs and HNCs photochemical systems.

